Journal of Applied Polymer Science

Effect of the ionic liquid [bmim]PF_6 on the nonisothermal crystallization kinetics behavior of poly(ether-*b*-amide)

Yunxiang Bai, Guoliang Wu, Qian Zhang, Chunfang Zhang, Jin Gu, Yuping Sun
The Key Laboratory of Food Colloids and Biotechnology, Ministry of Education, School of Chemical and Material Engineering, Jiangnan University, Wuxi 214122, People's Republic of China
Correspondence to: C. F. Zhang (E-mail: zcf326@163.com)

ABSTRACT: Blending ionic liquid with crystalline polymer permits the design of new high-performance composite materials. The final properties of these materials are critically depended on the degree of crystallinity and the nature of crystalline morphology. In this work, nonisothermal crystallization behavior of poly(ether-*b*-amide) (Pebax®1657)/room temperature ionic liquid (1-butyl-3-methylimidazolium hexafluorophosphate, [bmim]PF_6) was investigated by differential scanning calorimetry. The presence of [bmim]PF_6 can retard the nucleation of Pebax®1657 and lead to the crystallization depression of the PA block and the crystalline disappearance of the PEO block. However, the dilution effect of the IL results in a higher growth rate of crystallization of PA block. The influence of [bmim]PF_6 content and cooling rate on crystallization mechanism and spherulitc structures was determined by the Avrami equation modified by Jeziorny and Mo's methods, whereas the Ozawa's approach fails to describe the nonisothermal crystallization behavior of Pebax®1657/[bmim]PF_6 blends. In the modified Avrami analysis, the Avrami exponent of PA blocks, $n > 3$, for pure Pebax®1657, while $3 > n > 2$ for Pebax®1657/[bmim]PF_6 blends testifies the transformation of crystallization growth pattern induced by [bmim]PF_6 from three-dimensional growth of spherulites to a combination of two- and three-dimensional spherulitic growth. Further, lower activation energy for the nonisothermal crystallization of PA blocks of Pebax®1657 can be observed with the increase of [bmim]PF_6 content. © 2015 Wiley Periodicals, Inc. J. Appl. Polym. Sci. **2015**, *132*, 42137.

KEYWORDS: crystallization; ionic liquids; kinetics

Received 30 December 2014; accepted 22 February 2015
DOI: 10.1002/app.42137

INTRODUCTION

Crystalline polymers are quantitatively one of the most important products of the chemical industry used worldwide. To tune their physical structures to achieve the desired application properties, crystalline polymers have often been composited with various solid or liquid additives.[1] It has been widely reported that the final properties of blends are critically depended on the degree of crystallinity and the nature of crystalline morphology. Thus, it is of great significance to understand the impact of additives on the crystallization behaviors of these polymers.[2,3]

Ionic liquids (ILs), which are recognized as environment-friendly liquid additives, have attracted intensive attentions in several fields of chemical industry[4,5] owing to their good catalytic properties, excellent thermal stability, nonflammability, high ionic conductivity, and wide electrochemical window. In particular, the basic structural attribute of ILs is iconicity, favorable for stabilization of polymer chains via delocalized electrostatic interaction through charge, which originated some interesting polymer/IL blend systems.[6] Up to now, reports of the effects of ILs on the crystallization behaviors of crystalline polymer are quite limited. Dou and Liu[7] studied the isothermal and nonisothermal crystallization behaviors of poly(ethylene terephthalate)/IL composites. They found that pyrrolidinium ILs could serve as effective nucleating agents in accelerating the crystallization of poly(ethylene terephthalate). However, after studying the effect of ILs on the crystallization kinetics behavior of poly(ethylene oxide) (PEO), Chaurasia *et al.*[8] infer a completely opposite conclusion. They reported that the incorporation of IL would significantly slow down the melt crystallization rate of PEO owing to the interaction between IL and PEO chains. On the other hand, it was reported that ILs could influence not only the crystallization rate but also the crystal form of crystalline polymers. He *et al.*[9] incorporated four types of ILs into PVDF to form PVDF/IL composites. They found that ILs could act as a directing agent to facilitate the crystallization transformation process accompanied by the interference in crystal growth. The β-form crystalline phase of the PVDF component could be greatly improved just by incorporating a little amount of ILs.

Poly(amide-*b*-ether), commercialized under the trade name Pebax® (Arkema), is a versatile crystalline polymer in which polyether and polyamide were used as the soft and hard segments, respectively. Various grades of Pebax have been synthesized by varying the amide and ether composition for applications in a wide variety of products, such as virus-proof surgical equipments, food packaging materials, antistatic sheets or belts, films for textile lamination used in sports wears and gloves, and so forth.[10,11] Recently, ILs have been incorporated into Pebax to improve or meet some required properties for certain purposes. For example, Heitmann *et al.*[12] immobilized the ILs into Pebax to prepare the pervaporation membranes for recovery of *n*-butanol. Bernardo *et al.*[13] reported that Pebax/IL blend can be identified as a suitable CO_2-selective membrane material. Apparently, the addition of an IL is expected to significantly change Pebax's crystallization behavior, which would greatly influence the microstructure, properties, and performance of Pebax/IL blends. However, to our knowledge, the crystallization kinetics behavior of Pebax with an IL has not been reported so far in the literature.

Compared to the isothermal crystallization, the nonisothermal crystallization investigation is of considerable practical significance. So this paper reports the nonisothermal crystallization kinetics behavior of Pebax®1657 with different amounts of an IL, [bmim]PF_6. The choice of this particular IL in this study was governed principally by the following considerations: (a) [bmim]PF_6 is known to have the good compatibility with Pebax®1657,[13] which may produce significant changes in the chain flexibility and hence, the crystallization behavior; (b) [bmim]PF_6 can be available commercially in large volumes and has excellent thermal stability, which is vital for the study on crystallization kinetics. Nonisothermal crystallization kinetics was studied in this work using differential scanning calorimetry (DSC) and the experimentally measured kinetic values were available by means of a series of calculation procedures. The further purpose of this research was to gain insight into the influence of ILs on the thermal properties of Pebax®1657.

EXPERIMENTAL

Materials

Pebax®1657 containing 60 wt % of PEO and 40 wt % polyamide 6 (PA) was purchased from Arkema (Paris, France) and was used as received without further treatment. 1-Butyl-3-methylimidazolium hexafluorophosphate, [bmim]PF_6, was obtained from Shanghai Cheng Jie (Shanghai, China) and vacuum dried at 133 Pa for 24 h before used. *n*-Propanol, used as solvent, was supplied by National Pharmaceutical Group Chemical Reagent, China. The chemical structures of Pebax®1657 and [bmim]PF_6 are shown in Figure 1.

Preparation of Pebax®1657/[bmim]PF_6 Blends

Pebax®1657/[bmim]PF_6 blends with various [bmim]PF_6 content were prepared through solution casting method. In brief, Pebax®1657 was dissolved in a mixture of propanol/water (70/30 wt/wt) with a concentration of 10 wt % at room temperature. Then different amounts of [bmim]PF_6 were added into the above solution with stirring for 1–2 h until a clear homogeneous solution was obtained. The viscous solution

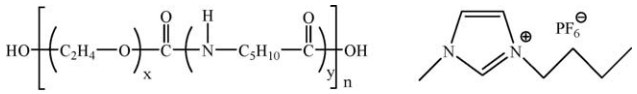

Figure 1. Chemical structure of Pebax®1657 and [bmim]PF_6.

was poured into a tetrafluoroethylene Petri dish. After complete evaporation of the solvent, Pebax®1657/[bmim]PF_6 blends containing different amounts of [bmim]PF_6 were obtained. These blends were further dried under vacuum before use.

Differential Scanning Calorimetry

A Mettler DSC 7 (STAR^e System, Mettler Toledo, Switzerland) differential scanning calorimeter, operated at 25 mL/min nitrogen flow, was used to detect the evolution of crystallization during the cooling process of Pebax®1657/[bmim]PF_6 blends. Temperature and heat flow were calibrated with indium standards. A dry and constant flow of nitrogen was maintained to eliminate thermal gradients and ensure the validity of the calibration standard from sample to sample. Every sample, 8 mg, was accurately weighted for DSC testing.

Before analyses, each sample was heated from room temperature to 200°C under the heating rate of 10°C/min. After maintaining at this temperature for 3 min to erase thermal history, the sample was then cooled to −50°C at four different cooling rates: 5, 10, 20, and 30°C/min. The exothermic curves of heat flow with temperature decreasing at various rates were recorded to analyze the nonisothermal crystallization process. The values of crystallization temperature (T_p) and enthalpy of crystallization ΔH (J/g) were calculated during the cooling runs.

Theoretical Basis of Nonisothermal Crystallization Kinetics

The nonisothermal crystallization kinetics of polymer are generally analyzed by the modification of Avrami equation based on the assumption that nonisothermal crystallization could be approximated by a sequence of infinitesimally small isothermal steps. Among these theoretical formulations, Avrami equation modified by Jeziorny, Ozawa equation and Mo method were adopted to describe the nonisothermal crystallization kinetics of Pebax®1657.

Avrami Equation Modified by Jeziorny[14]

Avrami equation modified by Jeziorny is a method based on the characteristics of nonisothermal processes and it assumes that nonisothermal crystallization with a fixed cooling rate comprises a series of infinite small isothermal crystallization steps. Hence, the kinetics of the overall nonisothermal crystallization rate is described as the following equation:

$$X_t = \frac{\int_{T_0}^{T} (dH_c/dT)dT}{\int_{T_0}^{T_\infty} (dH_c/dT)dT} = 1 - \exp(-Z_t t^n), \quad (1)$$

where X_t is the relative crystallinity at time t, T_0, T, and T_∞ are the onset crystallization temperature at $t = 0$, the crystallization

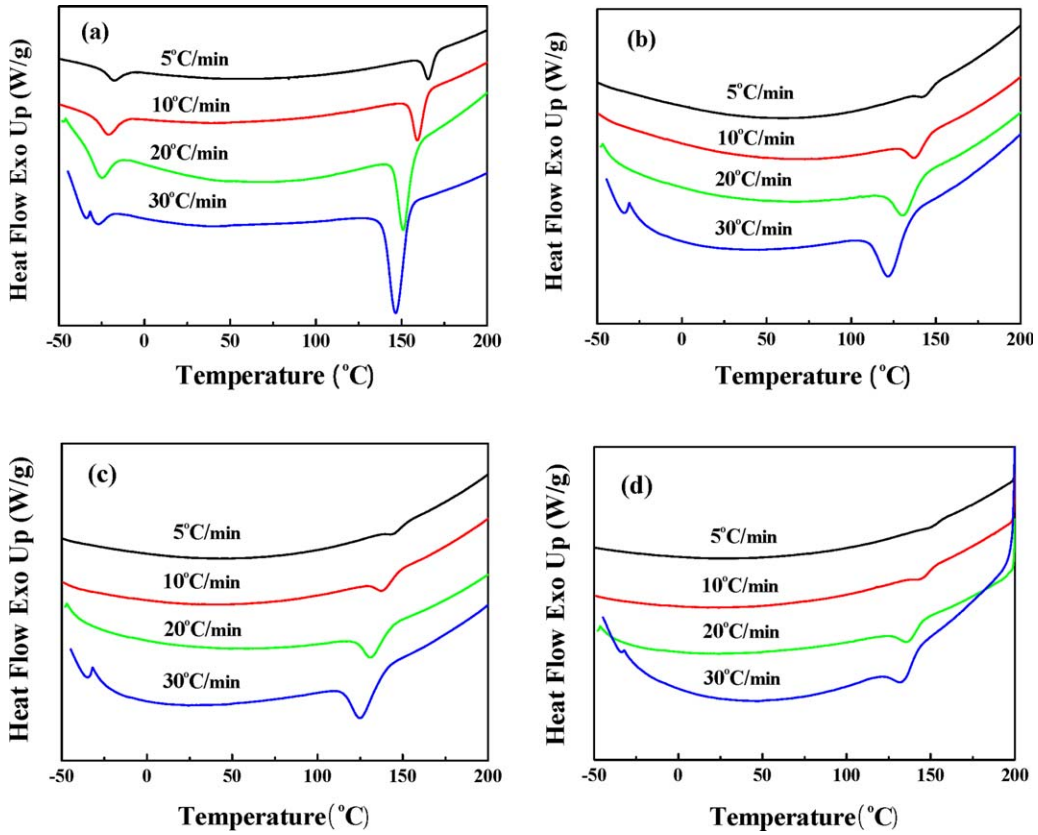

Figure 2. DSC curves of Pebax®1657/[bmim]PF_6 blends with different [bmim]PF_6 content during nonisothermal crystallization. (a) 0 wt %, (b) 20 wt %, (c) 40 wt %, and (d) 60 wt %. [Color figure can be viewed in the online issue, which is available at wileyonlinelibrary.com.]

temperature at $t = t$, and the end crystallization temperature at the complete crystallization, respectively. dH_c is the enthalpy of crystallization during time interval dT, Z_t is the overall crystallization rate constant containing the processes of nucleation and growth, n is the Avrami exponent depending on the mechanism of nucleation as well as the growth geometry.

In nonisothermal crystallization, time t can be related to temperature T as follows:

$$t = \frac{T_O - T}{\Phi}, \tag{2}$$

where Φ is the cooling rate.

By taking natural logarithms, eq. (1) can be expressed as follows:

$$\lg[-\ln(1-X_t)] = n\lg t + \lg Z_t. \tag{3}$$

According to eq. (3), Z_t and n can be obtained from the slop and intercept of the straight lines obtained by plotting lg $[-\ln(1 - X_t)]$ versus lg t. Assuming the influence of the cooling rate for nonisothermal crystallization, the final form of the rate constant (Z_t) should be corrected as follows:

$$\lg Z_c = \frac{\lg Z_t}{\Phi}, \tag{4}$$

where Z_c is the kinetics crystallization rate constant of nonisothermal crystallization rectified by cooling rate Φ as the calibration factor.

Ozawa Equation[15,16]

Considering the influence of the cooling rate, the Ozawa equation for nonisothermal crystallization has been adapted and takes the form

$$X_T = 1 - \exp[-K_T/\Phi^m], \tag{5}$$

where X_T is the relative crystallinity at a temperature T, K_T is the crystallization rate function which is related to the geometry of nucleation and the crystallization rate, Φ is the cooling rate, m is the Ozawa exponent representing the dimensionality of crystal growth and the mode of nucleation. Equation (5) can be rearranged by taking logarithms on both sides:

$$\lg[-\ln(1-X_T)] = \lg K_T - m\lg\Phi. \tag{6}$$

Plots of lg $[-\ln(1 - X_T)]$ against lg Φ give straight lines with a slope of $-m$ and an intercept of lg K_T.

Mo Method[17]

To describe exactly the nonisothermal crystallization process, Mo and coworkers incorporated the Avrami equation and the Ozawa equation, and obtained the function of Φ versus t at a given crystallinity. It can be expressed as:

$$\lg Z_t + n\lg t = \lg K(T) - m\lg\Phi \tag{7}$$

$$\lg\Phi = \lg F(T) - \alpha \tag{8}$$

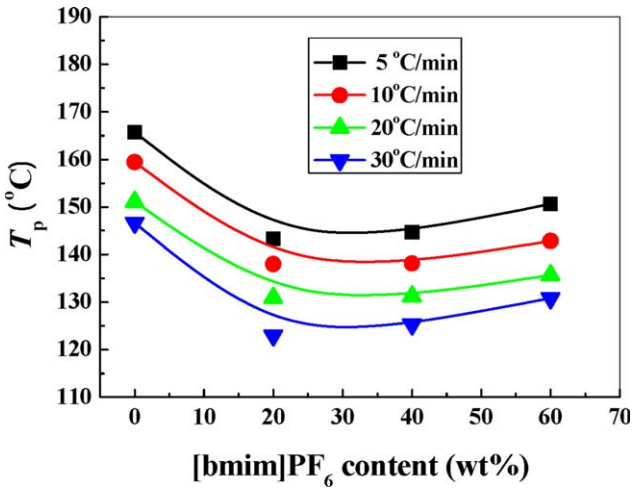

Figure 3. T_p of PA blocks of Pebax®1657 at different [bmim]PF_6 content during nonisothermal crystallization. [Color figure can be viewed in the online issue, which is available at wileyonlinelibrary.com.]

$$F(T)=[K(T)Z_t]^{1/m}, \tag{9}$$

where the kinetics parameters $F(T)$ is the cooling rate required to reach a defined degree of crystallinity at unit crystallization time, and the Mo index α is ratio of the Avrami index to that of Ozawa, i.e., $\alpha = n/m$ and is related to the mechanism of nucleation and crystal growth. The parameters α and $F(T)$ can be obtained from plots of lg Φ versus lg t at a defined relative crystallinity from the slope of $-\alpha$ and intercept of lg $F(T)$.

Activation Energy of Nonisothermal Crystallization

The activation energy of nonisothermal crystallization can be determined using the Kissinger equation:[18]

$$\frac{d\left[\ln\left(\Phi/T_p^2\right)\right]}{d(1/T_p)}=-\frac{\Delta E}{R}, \tag{10}$$

where ΔE is the activation energy for crystallization, R is the gas constant, Φ is the cooling rate, and T_p is the temperature at the maximum exothermic peak. ΔE was obtained from the slope of the plot of $\ln[\Phi/T_p^2]$ versus $1/T_p$.

RESULTS AND DISCUSSION

Thermal Behavior of Pebax®1657/[bmim]PF_6 Blends in Nonisothermal Conditions

Figure 2 shows the DSC curves of pure Pebax®1657 and Pebax®1657/[bmim]PF_6 blends recorded as the change of heat flow with the decreasing temperature at different cooling rates. [bmim]PF_6 crystallization cannot be considered in the cooling curves owing to the low melting points and high supercooling degrees. In the DSC curve of pure Pebax®1657, two dominant endothermic peaks are present, whose maxima occur approximately at -20 and 150°C. These endotherms

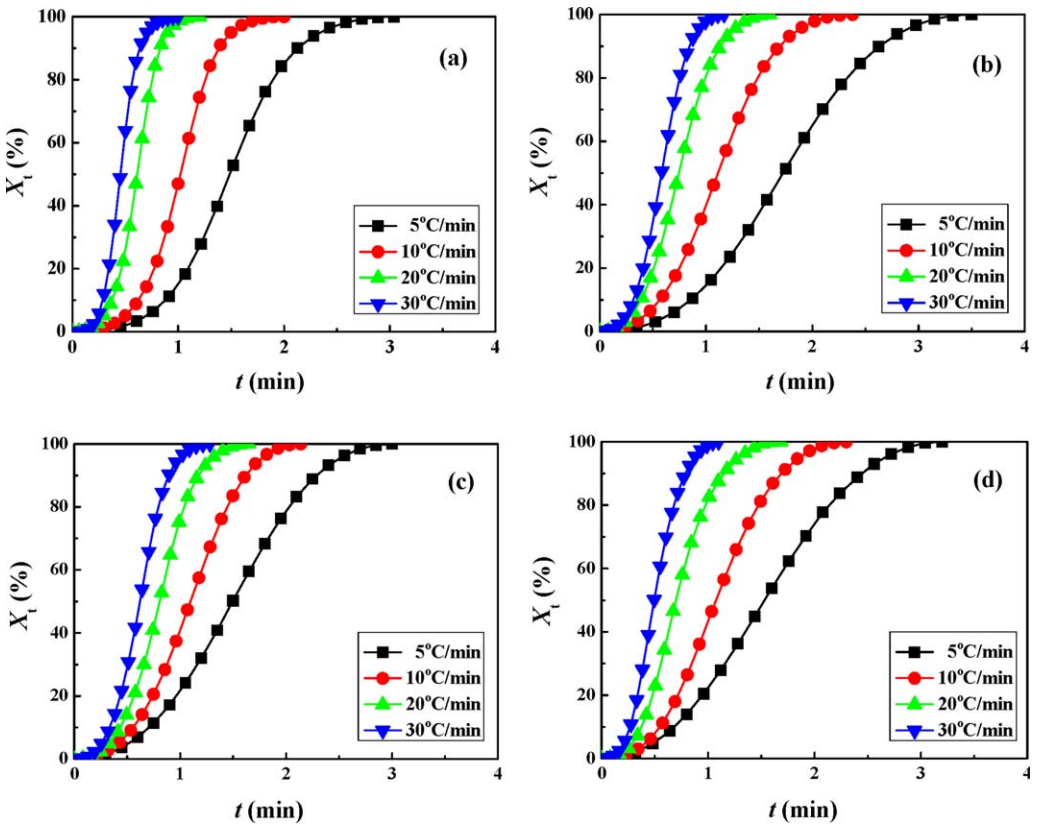

Figure 4. Development of relative crystallinity X_t with crystallization time t for PA blocks of Pebax®1657 with different [bmim]PF_6 content. (a) 0 wt %, (b) 20 wt %, (c) 40 wt %, and (d) 60 wt %. [Color figure can be viewed in the online issue, which is available at wileyonlinelibrary.com.]

Table I. Half-Time of Crystallization, $t_{1/2}$ (min), in the Nonisothermal Process at Different Cooling Rates for Pebax®1657/[bmim]PF_6 Blends

[bmim]PF_6 content (wt %)	Cooling rate (°C/min)			
	5	10	20	30
0	1.49	1.06	0.69	0.48
20	1.53	1.10	0.74	0.59
40	1.49	1.10	0.79	0.61
60	1.53	1.08	0.75	0.54

Table II. The Values of X_s (%) for Pebax®1657/[bmim]PF_6 Blends at Different Cooling Rates

[bmim]PF_6 content (wt %)	Cooling rate (°C/min)			
	5	10	20	30
0	15	12	13	14
20	—	22	22	23
40	—	—	26	25
60	—	40	36	34

"—" express that the values of X_s cannot be calculated from Figure 5 owing to the inconspicuous inflexion.

can be attributed to the crystalline fraction of the blocks of PEO and PA, respectively. However, in the Pebax®1657/[bmim]PF_6 blends, the crystallization peak of PEO disappears completely. Furthermore, with the addition of [bmim]PF_6, the strong and relatively sharp endothermic peak of the crystalline PA blocks is replaced by a much weaker and broader melting one, which suggesting a reduction of the average crystal size and/or purity.

Crystallization peak temperatures (T_p) of PA blocks obtained from the DSC curves are presented in Figure 3. It is evident that [bmim]PF_6-containing samples have lower T_p values than pure Pebax®1657. This result indicated that the presence of [bmim]PF_6 can weaken the nucleation of PA blocks. When [bmim]PF_6 content was higher than 20 wt %, T_p values of PA block increased slightly. We speculated that the higher crystallization temperatures of PA segments at higher IL content arose from the connected amorphous PEO block. Chain folding of the crystallizable PA segment in the block copolymers led to the deformation of the amorphous PEO block to some extent, which required the conformational rearrangement of the amorphous block during crystallization. At higher [bmim]PF_6 content, the faster conformational rearrangement of the amorphous PEO block promoted crystallization of the PA segment, and this led to a higher crystallization temperature.

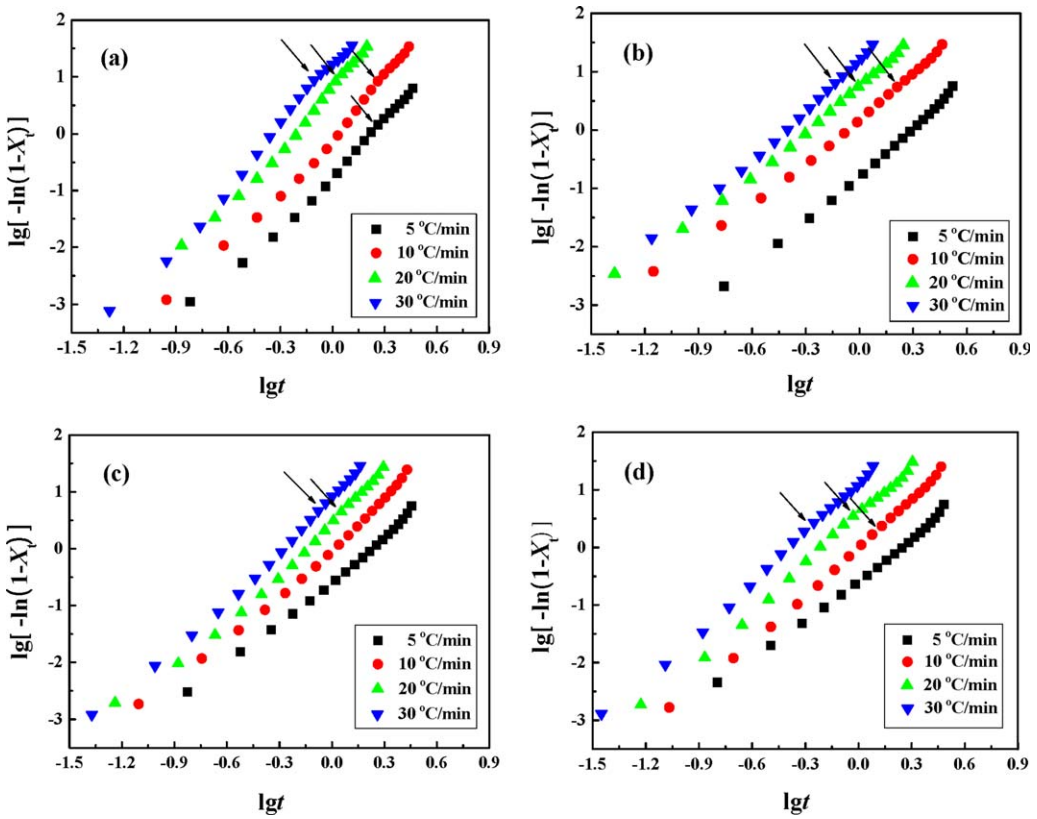

Figure 5. The plots of lg $[-\ln(1-X_t)]$ versus lg t for Pebax®1657/[bmim]PF_6 blends: (a) 0 wt %, (b)20 wt %, (c) 40 wt %, and (d) 60 wt % at different cooling rates. The arrows show the inflection point from the primary crystallization stage to the secondary crystallization stage. [Color figure can be viewed in the online issue, which is available at wileyonlinelibrary.com.]

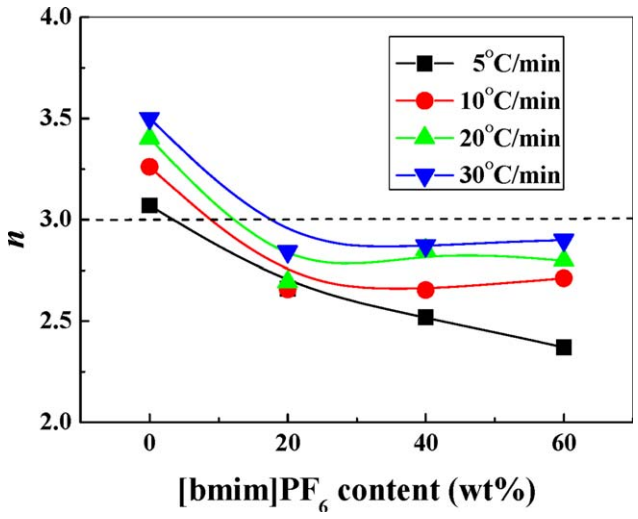

Figure 6. The values of n for PA blocks of Pebax®1657 with different [bmim]PF_6 content during the nonisothermal crystallization. [Color figure can be viewed in the online issue, which is available at wileyonlinelibrary.com.]

Furthermore, lower T_p of PA blocks of Pebax®1657 observed as the cooling rate rises at a fixed [bmim]PF_6 content. This phenomenon is typical and common for the most semicrystalline polymer in their nonisothermal crystallization process. When PA block crystallized at a lower cooling rate, there was a relatively long time remaining within the temperature range that promoted sufficient mobility of PA segments, which is in favor of the growth of crystallites. When cooled at a relatively rapid rate, however, the polymer segments were "frozen" before the formation of regular crystallites, thus decreasing the crystallization temperature T_p.

According to eq. (1), the relative crystallinity (X_t) for PA blocks of Pebax®1657 with different [bmim]PF_6 content is plotted as a function of time t at different cooling rates. The values are given in Figure 4. It can be seen that all the samples show sigmoid characteristics and shift toward a shorter time scale region as the cooling rate increased. These features indicate that the crystallization rate of PA blocks becomes faster at a higher cooling rate and the samples crystallize more rapidly.

Crystallization half-time, $t_{1/2}$, which is regarded as a very important crystallization kinetic parameter, is defined as the time necessary to attain 50% relative crystallinity. Usually, $t_{1/2}$ is used to characterize the crystallization rate directly. That is, the larger the value of $t_{1/2}$, the lower the crystallization rate.[19] Table I summarizes the values of $t_{1/2}$ (read directly from Figure 4) for PA blocks of pure Pebax®1657 and Pebax®1657/[bmim]PF_6 blends. It is remarkable that $t_{1/2}$ is close to constant with the increase of the IL concentration at a given cooling rate. Generally, the overall crystallization rate is controlled by two factors, namely, nucleation and growth. On one hand, the addition of [bmim]PF_6 into Pebax®1657 can retard the nucleation of PA blocks (as is stated above), which leads to a lower nucleation rate. On the other hand, the dilution effect of the IL results in a higher crystal growth rate of PA blocks. Comparatively, in the studied IL concentration range, these two effects were exactly offset, which caused the crystallization rate changed slightly. Additionally, the increase of cooling rate can raise the nucleation density and reduce the crystal growth rate of PA blocks.[20] In this case, the effect of the latter is more dominant to promote the crystallization rate, which results in the enhancement of crystallization rate.

Nonisothermal Crystallization Kinetics According to the Avrami Equation Modified by Jeziorny

According to eqs. (2) and (3), the characteristics of nonisothermal crystallization kinetics for pure Pebax®1657 and Pebax®1657/[bmim]PF_6 blends were analyzed by the Avrami equation modified by Jeziorny. Figure 5 illustrates the plot of lg $[-\ln(1-X_t)]$ versus lg t for different Pebax®1657/[bmim]PF_6 blends at different cooling rates. It can be seen that most of the curve show the initial linear portion and then level off. This deviation compartmentalizes the whole crystallization process into two stages, a primary and secondary crystallization process. The primary crystallization process consists of the radial growth of the crystallites until impingement and the secondary crystallization involves the growth or subsidiary lamellae or lamella thickening within the crystallites in the later stage of isothermal crystallization process.[21] Therefore, secondary crystallization as a source of structural evolution is closely relative to the mechanical strength of polymer materials. The percentage of secondary crystallization in total crystallinity, X_s, can be defined according to the following equation:[22]

$$X_S = 1 - X_P, \tag{11}$$

where X_p is the relative crystallinity at the end of the primary process. Table II illustrates the variation of X_s for Pebax®1657/[bmim]PF_6 blends with various [bmim]PF_6 content during the nonisothermal crystallization. It can be seen that the extent of secondary crystallization for pure Pebax®1657 is relatively small (about 13%). However, it increases dramatically with the enhancement of the IL content and reaches about 37% for Pebax®1657/[bmim]PF_6 blends with 60 wt % [bmim]PF_6 content. The relatively high content of secondary crystallization at higher [bmim]PF_6 content can be attributed to the higher mobility of PA blocks of Pebax®1657. As we know that the diffusion of PA chains toward the crystallization growth front will become easy and frequent with the increase of [bmim]PF_6 content. Therefore, a great part of crystallizable chains, which did not incorporate into crystallites at primary crystallization, is more prone

Table III. The Values of Z_c for Pebax®1657/[bmim]PF_6 Blends at Different Cooling Rates

[bmim]PF_6 content (wt %)	Cooling rate (°C/min)			
	5	10	20	30
0	0.942	0.993	1.006	1.014
20	0.946	0.989	1.004	1.008
40	0.953	0.991	1.003	1.007
60	0.953	0.990	1.005	1.011

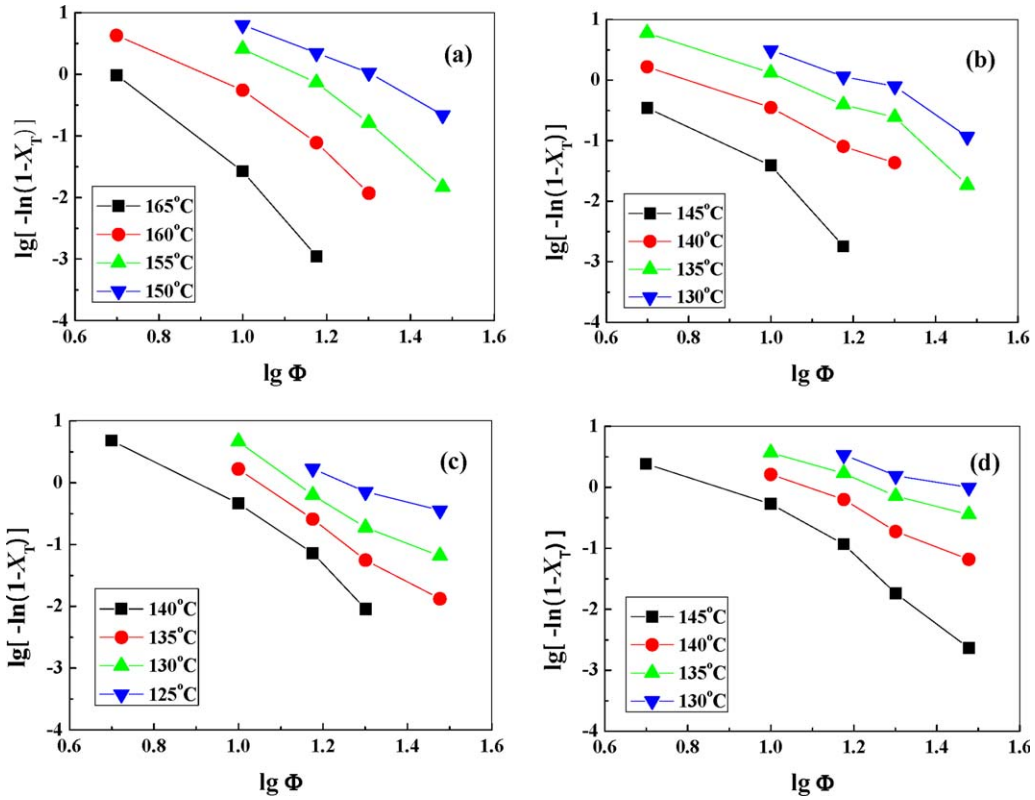

Figure 7. Ozawa plots for nonisothermal crystallization of Pebax®1657/[bmim]F_6 blends with different [bmim]F_6 content: (a) 0 wt %, (b) 20 wt %, (c) 40 wt %, and (d) 60 wt %. [Color figure can be viewed in the online issue, which is available at wileyonlinelibrary.com.]

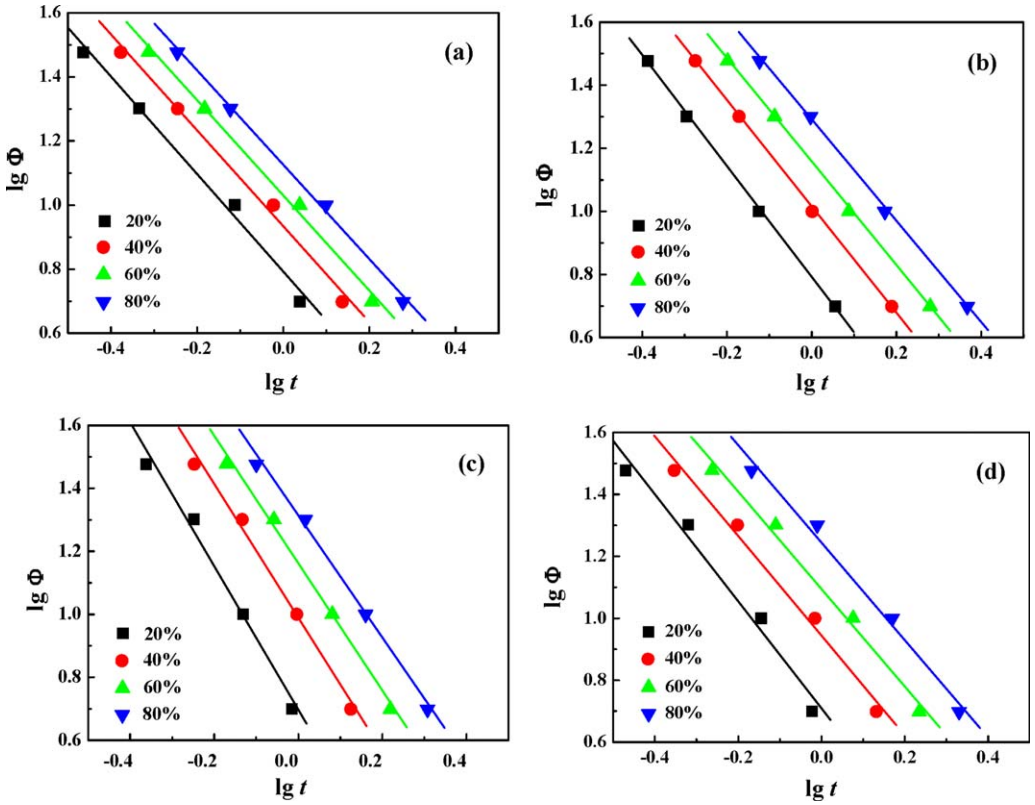

Figure 8. Plots of log Φ versus lg *t* from the Mo's method for nonisothermal crystallization of Pebax®1657/[bmim]PF_6 blends with different [bmim]PF_6 content: (a) 0 wt %, (b) 20 wt %, (c) 40 wt %, and (d) 60 wt %. [Color figure can be viewed in the online issue, which is available at wileyonlinelibrary.com.]

Table IV. The Values of $F(T)$ (°C/min) and α for PA Blocks of Pebax®1657 with Different [bmim]PF_6 Contents

[bmim]PF_6 content (wt %)	Relative crystallinity X_t (%)							
	20		40		60		80	
	$F(T)$	α	$F(T)$	α	$F(T)$	α	$F(T)$	α
0	6.20	1.52	8.59	1.49	12.72	1.48	17.36	1.47
20	6.20	1.76	9.39	1.68	14.42	1.64	19.59	1.61
40	5.97	2.28	9.77	2.12	14.54	2.02	19.64	1.94
60	5.61	1.73	8.80	1.61	12.43	1.57	18.55	1.57

to crystallize into thinner less-perfect lamellar during secondary crystallization, and leads to the enhancement of the secondary crystallization content accordingly.

Fitting the straight line of lg $[-\ln(1-X_t)]$ versus lg t at the primary crystallization stage allows us to determine n and Z_c in nonisothermal crystallization, and the values are listed in Figure 6 and Table III. The values of n for PA blocks of pure Pebax®1657 range from 3.1 to 3.5. This result indicates that heterogeneous nucleation and three-dimensional growth of spherulites were formed during the nonisothermal crystallization processes. Qu *et al.*[23] and Liu *et al.*[24] studied the nonisothermal crystallization kinetics of PA 6 and PA 11, respectively. They found that the values of n at the primary crystallization stage range from 4.0 to 4.7 for PA 6 and from 5.1 to 7.7 for PA 11, respectively. In our study, the diffusion of PA chains toward the crystallization growth front would be restrained by the conjoined amorphous PEO blocks. The relatively low mobility of PA segments would prevent the PA blocks from crystallizing through a more complicated mechanism, which results in a low value of n. For Pebax®1657/[bmim]PF_6 blends, the values of n are between 2.4 and 2.9, suggesting that the crystallization of PA blocks proceeds by a hybrid crystal structure of planar lamellae and three-dimensional spherulitic growth in the presence of [bmim]PF_6. In addition, Pebax®1657/[bmim]PF_6 blends with 60 wt % [bmim]PF_6 content at 2°C/min cooling rate have the lowest values of n, indicating that the strong polarity of the IL significantly prevents the spherulites from their full development at low cooling rate.

The reason for the diversity of n is the variation in cooling rate. Generally, the relationship between n and Φ is linear, i.e., the more the value of n, the more significant the athermal nucleation.[7] In this case, there has no obvious linear relationship between n and Φ, demonstrating that thermal nucleation is the main pattern for PA block of pure Pebax®1657 and Pebax®1657/[bmim]PF_6 blends in nonisothermal crystallization processes. The similar results were also reported in polyazomethine/MC nylon composites.[23]

The values of Z_c of Pebax®1657 and Pebax®1657/[bmim]PF_6 blends are expected to increase as the cooling rate increases, while the diversities are inconspicuous at different amounts of the IL under the same cooling rate. These results are congruent with observations made on $t_{1/2}$ above. Nonisothermal crystallization kinetics according to the Ozawa equation.

According to eq. (6), lg $[-\ln(1-X_T)]$ versus lg Φ plots for PA blocks of Pebax®1657 with different [bmim]PF_6 content are shown in Figure 7. Clearly, these straight lines do not exhibit a parallel relationship, which makes it very difficult to determine the constant value of m. For the Ozawa equation, it is impossible to predict the nucleation mechanism occurring during nonisothermal crystallization from a wide range of m values. Such findings are also observed in the systems of polyamide[24] and polyethylene.[25] The inapplicability of the Ozawa equation can be attributed to three main factors: the Ozawa analysis does not take into consideration of secondary crystallization process; the Ozawa exponent may change with the crystallization temperature, the cooling rate, and the transformed volume function; during the plotting lg $[-\ln(1-X_T)]$ against lg Φ, it is very difficult to get a precise straight line only from two or three points at a given temperature. Consequently, the Ozawa equation fails to provide a suitable description for the nonisothermal crystallization of PA block of Pebax®1657 with or without [bmim]PF_6.

Nonisothermal Crystallization Kinetics According to the Mo Method

Another theoretical prediction proposed by Mo is also used to describe the nonisothermal crystallization of

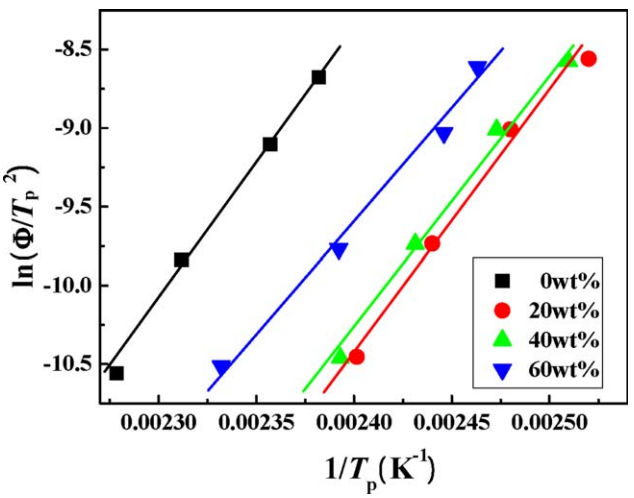

Figure 9. Determination of the activation energy by plotting ln (Φ/T_P^2) versus $1/T_P$ based on the Kissinger equation. [Color figure can be viewed in the online issue, which is available at wileyonlinelibrary.com.]

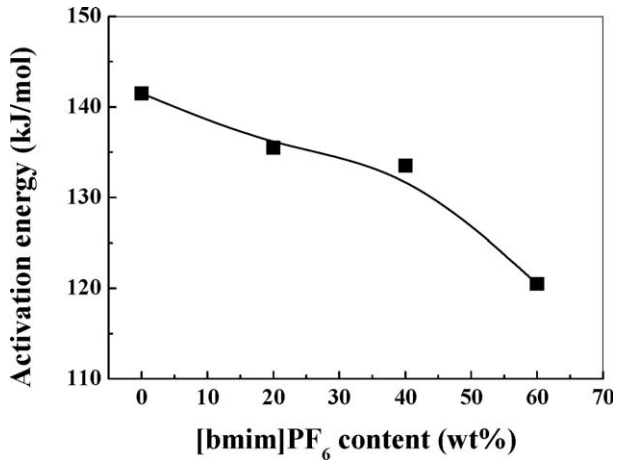

Figure 10. Curves of activation energy versus [bmim]PF_6 content.

Pebax®1657/[bmim]PF_6 blends for comparison. Examining the linear relationship between lg Φ and lg t at a given relative crystallinity (20, 40, 60, and 80%, Figure 8) implies agreement between the experimental data and the theoretical predictions for pure Pebax®1657 and Pebax®1657/[bmim]PF_6 blends. The values of α and $F(T)$ are tabulated in Table IV.

It can be seen that the values of $F(T)$ increase systematically with increasing relative crystallinity for both pure Pebax®1657 and Pebax®1657/[bmim]PF_6 blends. In the Mo method, the physical meaning of $F(T)$ is the cooling rate required to reach a defined degree of crystallinity at the unit crystallization time. The smaller the value of $F(T)$, the higher the crystallization rate. Therefore, this result indicates that within unit crystallization time a higher cooling rate should be required to achieve a higher degree of crystallinity. At the same crystallinity, the value of $F(T)$ of Pebax®1657/[bmim]PF_6 blends is similar with that of pure Pebax®1657, indicating that to reach the same relative degree of crystallinity X_t, the crystalline time for PA block in Pebax®1657/[bmim]PF_6 is equal to that in pure Pebax®1657. This result is in good agreement with the above result from $t_{1/2}$ and the Avrami equation modified by Jeziorny.

The values of α are close to constant at different relative crystallinities and have the maximum values at 40 wt % [bmim]PF_6 content. The change in α indicates that differences exist in aspects of the mechanism of nucleation and crystal growth with different IL contents.

Activation Energy of Nonisothermal Crystallization

The plot of $\ln[\Phi/T_p^2]$ versus $1/T_p$ and the relationship between ΔE and [bmim]PF_6 content are shown in Figures 9 and 10. According to Figure 10, lower activation energy for the nonisothermal crystallization of PA blocks of Pebax®1657 is observed as [bmim]PF_6 content rises. ΔE is the activation energy required to transport molecular segments to the crystallization surface.[17] A lower ΔE of PA blocks of Pebax®1657/[bmim]PF_6 blends suggests a higher crystallization growth ability compared with pure Pebax®1657 due to the diluent effect of IL.

CONCLUSIONS

The effect of IL, [bmim]PF_6, content on the nonisothermal crystallization behavior of Pebax®1657 has been investigated by means of DSC technique. The crystallization kinetics behaviors of Pebax®1657/[bmim]PF_6 blends were investigated systematically. The Avrami equation modified by Jeziorny and Mo's method was found to be able to effectively describe nonisothermal crystallization process of Pebax®1657/[bmim]PF_6 blend. The value of the Avrami exponent n of PA blocks for pure Pebax®1657 ranges from 3.1 to 3.5, while the values of n for Pebax®1657/[bmim]PF_6 blend are between 2.4 and 2.9. The values of $F(T)$ by the Mo's method suggested that the crystallization rate of PA blocks is closely constant with variation of the IL content. The activation energy of nonisothermal crystallization by the Kissinger equation showed that the crystallization ability increased with increasing [bmim]PF_6 content.

ACKNOWLEDGMENTS

This research was financially supported by the National Nature Science Foundation of China (21106053) and the Industry-Academia-Research Joint Research Project of Jiangsu Province (BY2013015-28).

REFERENCES

1. Sapuan, S. M.; Mansor, M. R. *Mater. Des.* **2014**, *58*, 161.
2. Quan, H.; Li, Z. M.; Yang, M. B.; Rui, H. *Compos. Sci. Technol.* **2005**, *65*, 999.
3. Ning, N. Y.; Fu, S. R.; Zhang, W.; Chen, F.; Wang, K.; Deng, H.; Zhang, Q.; Fu, Q. *Prog. Polym. Sci.* **2012**, *37*, 1425.
4. Kim, K. S.; Choi, S.; Demberelnyamba, D.; Lee, J. *Chem. Commun.* **2014**, *7*, 828.
5. Yeon, S. H.; Kim, K. S.; Choi, S.; Cha, J. H.; Lee, H. *J. Phys. Chem. B.* **2014**, *109*, 856.
6. Reed, S. K.; Lanning, O. J.; Madden, P. A. *J. Chem. Phys.* **2007**, *126*, 084704/1.
7. Dou, J. Y.; Liu, Z. P. *Polym. Int.* **2013**, *62*, 1698.
8. Chaurasia, S. K.; Singh, R. K.; Chandra, S. *Cryst. Eng. Comm.* **2013**, *15*, 6022.
9. He, L. H.; Sun, J.; Wang, X. X.; Wang, C. D.; Song, R.; Hao, Y. M. *Polym. Int.* **2013**, *62*, 638.
10. Hoffendahl, C.; Fontaine, G.; Bourbigot, S. *Polym. Degrad. Stab.* **2013**, *98*, 1247.
11. Kamal, T.; Park, S. Y.; Choi, M. C.; Chang, Y. W.; Chuang, W. T.; Jeng, U. S. *Polymer* **2012**, *53*, 3360.
12. Heitmann, S.; Krings, J.; Kreis, P.; Lennert, A.; Pitner, W. R.; Górak, A.; Schulte, M. M. *Sep. Purif. Technol.* **2012**, *97*, 108.
13. Bernardo, P.; Jansen, J. C.; Bazzarelli, F.; Tasselli, F.; Fuoco, A.; Friess, K.; Izák, P.; Jarmarová, V.; Kačírková, M.; Clarizia, G. *Sep. Purif. Technol.* **2012**, *97*, 73.
14. Jeziorny, A. *Polymer* **1978**, *19*, 1142.
15. Ozawa, T. *Polymer* **1971**, *2*, 150.
16. Ozawa, T. *J. Therm. Anal. Calorim.* **1976**, *9*, 369.

17. Liu, T. X.; Mo, Z. S.; Zhang, H. F. *J. Appl. Polym. Sci.* **1998**, *67*, 815.
18. Kissinger, H. E. *Anal. Chem.* **1957**, *29*, 1702.
19. Qian, J. S.; He, P. S.; Nie, K. M. *J. Appl. Polym. Sci.* **2004**, *91*, 1013.
20. Zhang, C. F.; Zhu, B. K.; Ji, G. L.; Xu, Y. Y. *J. Appl. Polym. Sci.* **2006**, *99*, 2782.
21. Jenkins, M. J.; Harrison, K. L. *Polym. Adv. Technol.* **2006**, *17*, 474.
22. Zhang, C. F.; Bai, Y. X.; Gu, J.; Sun, Y. P. *J. Appl. Polym. Sci.* **2011**, *122*, 2442.
23. Qu, X. W.; Ding, H. L.; Lu, J. Y.; Wang, Y. X.; Zhang, L. C. *J. Appl. Polym. Sci.* **2004**, *93*, 2844.
24. Liu, S. Y.; Yu, Y. N.; Cui, Y.; Zhang, H. F.; Mo, Z. S. *J. Appl. Polym. Sci.* **1998**, *70*, 2371.
25. Eder, M.; Wlochowicz, A. *Polymer* **1983**, *24*, 1593.